Effect of Bismuth on Weld Joint Penetration in Austenitic Stainless Steel

Bismuth is shown to have a distinct effect on bead shape and joint penetration

BY Y. TAKEUCHI, R. TAKAGI AND T. SHINODA

ABSTRACT. Bismuth-added stainless steels have been developed due to their good machinability, with excellent chip fragmentation property in particular, and their superior characteristics of forging. Bismuth has been reported to act as a surface active agent that lowers the surface tension of molten metal and thus refines the solidification structure of cast ingots.

The effect of bismuth on the weldability of stainless steels is yet to be made clear. The effect of surface tension on the weld joint penetration shape of stainless steel in the case of gas tungsten arc welding has been extensively studied and clarified. In this work, the weldability of several specially prepared heats of 18-8 austenitic stainless steel containing varying additions of bismuth has been studied, with special attention being paid to clarifying the effect of bismuth on weld bead formation and weld penetration shape.

Bismuth acts as a surface active element and causes Marangonian convective flow to occur within the molten pool. Due to the positive temperature coefficient, deep penetration occurs, and there is a tendency for irregular bead formation.

Introduction

Austenitic stainless steels in general suffer from the drawback of poor machinability. Free-cutting stainless steels with improved machinability through the addition of elements such as sulfur, selenium or lead have been developed. However, in free-cutting stainless steels containing sulfur, lowering of corrosion resistance is unavoidable (Ref. 1). On the other hand, in the case of free-cutting stainless steels with selenium or lead additions, the toxic nature of these two elements in the dissolved state brings about limitations in the places or locations of use for such steels (Ref. 2).

With this as the background, bismuth, which is a nontoxic element, has received attention as a potential candidate for imparting free-cutting ability, and such stainless steels with bismuth additions have already been developed (Refs. 3, 4). At present, stainless steels containing 0.05 to 0.15% bismuth are beginning to be used for practical applications. Bismuth-added stainless steels have good machinability, with excellent chip fragmentation property in particular, and superior characteristics of forging. The corrosion resistance is known to be as good as those of AISI 304 steel (Ref. 5). In addition, bismuth has been reported to act as a surface active agent, which lowers the surface tension of molten metal and thus refines the solidification structure of cast ingots (Ref. 6).

The utilization of free-cutting stainless steels for machine construction involves not only machined components, but also welded assemblies. Generally, elements that impart free-cutting ability are said to cause deterioration in weldability because of high-temperature embrittlement. However, the effect of bismuth on the weldability of stainless steels is yet to be made clear. Also, in recent years, the effect of surface tension on the weld joint penetration shape of stainless steel in case of gas tungsten arc (GTA) welding has been extensively studied and clarified (Refs. 7–9).

Thus, if bismuth is a surface active element (Ref. 6), it is to be expected that bismuth addition would have a significant effect on the weldability of stainless steel, the weld joint penetration shape in particular.

In this work, the weldability of several specially prepared heats of 18-8 austenitic stainless steel containing varying additions of bismuth has been studied, with special attention being paid to clarify the effect of bismuth on weld bead formation and weld joint penetration shape.

KEY WORDS

Bismuth
Weld Joint Penetration
Austenitic Stainless
Stainless Steel
GTAW
Surface Tension
Bead Formation
Weldability
Marangoni Flow
Penetration Shape

Experiment

Materials

The chemical compositions of the specially prepared heats (A to E) of AISI 304 type austenitic stainless steel are shown in Table 1. Heats A and B are steels without any intentional additions of bismuth, having sulfur contents of 0.001% and 0.030%, respectively. In heats C, D and E, the sulfur content has been kept constant at 0.001%, and bismuth additions of 0.04 to 0.14% have been made.

The cast ingots were forged into two types of test specimens. The first type of 150 (l) X 50 mm (w) specimens (6 X 2 in.) with uniform thicknesses of either 9 or 15 mm (0.35 or 0.6 in.) (Fig. 1), were used to examine the weld joint penetration shapes and bead appearances. The other type consisted of tapered specimens of thicknesses varying continuously from 2 to 5 mm (0.08 to 0.2 in.) as shown in Fig. 2. These were used to measure the surface tension of the molten pool as will be described later.

Y. TAKEUCHI is Chief Research Engineer and R. TAKAGI is Manager, Metallurgical Service Section, Daido Steel Co. Ltd., Nagoya, Japan. T. SHINODA is Associate Professor, Material Processing Engineering Department, Nagoya, Japan.

Table 1—Chemical Compositions of Base Metals (wt-%)

Test plate	C	Si	Mn	P	S	Ni	Cr	Bi	Al
Steel: A (AISI 304)	0.07	0.25	1.87	0.030	0.001	8.42	18.12	<0.01	0.032
Steel: B (AISI 304)	0.02	0.26	1.75	0.034	0.030	8.29	18.83	<0.01	0.005
Steel: C (AISI 3048i)	0.06	0.21	1.92	0.030	0.001	8.64	18.41	0.04	0.022
Steel: D (AISI 3048i)	0.07	0.20	1.93	0.028	0.001	8.44	18.33	0.12	0.032
Steel: E (AISI 304Bi)	0.07	0.20	1.91	0.029	0.001	8.47	18.24	0.14	0.024

Table 2—Welding Parameters

Welding Procedure	Welding Current (A)	Electrode-Base Metal Distance (mm)	Welding Speed (cm/min)	Shielding Gas (L/min)
GTAW spot	150	3	0 arc time 8 s	Ar 10
Bead-on- plate (9 or 14 mm thick)	100–200	3	10–50	Ar 10
Bead-on-plate (Tapered plate)	200	3	10-50	Ar 10

Welding Conditions

Gas tungsten arc bead-on-plate welding was performed on specimens with varying bismuth contents, and the bead width, weld penetration shape and the state of bead formation were observed. The GTA welding equipment used consisted of a 300-A thyristor power source connected to a GTA welding torch, which was mounted on a fully automated welding robot. A 2.4-mm (0.09-in.) diameter thoriated tungsten electrode (2% Th) was used, and the electrode-to-work distance was maintained constant at 3 mm (0.12 in.). The shielding gas was argon, flowing at 10 L/min (4.7 ft^3/h). The welding current was varied from 100 to 200 A, and the welding speed from 10 to 50 cm/min (4 to 20 in./min) as shown in Table 2.

Arc Spot Welding Experiments

With the GTA torch held stationary, arc spot welds were made on the specimens in order to study the effect of bismuth content on the weld diameter and joint penetration shape. For this series of experiments, the welding current and arc time were kept constant at 150 A and 8 s, respectively. The weld diameter and penetration shape were observed by sectioning the welds.

Bead-on-Plate Welding Experiments

The welding conditions for the bead-on-plate welding experiments were mentioned earlier. The effect of bismuth on bead formation was studied by comparing the bead appearances and weld penetration shapes of bead cross-sections.

Measurement of Surface Tension

The variations in weld geometry, particularly the aspect ratio (*i.e.*, weld penetration/bead width) observed in the arc spot and bead-on-plate experiments, suggested that these may be caused by variations in the surface tension of the molten pool due to the presence of sulfur and bismuth. In order to measure the surface tension of the molten metal, a simple method suggested by Inagaki and Okada (Refs. 10, 11) was adopted. The principle of this method is shown in Fig. 2. This procedure was a quite simplified procedure to determine the surface tension as compared to conventional methods of levitated droplet or contact angle, if some experimental errors are permitted.

Using a tapered specimen, GTA welding was done from the thicker toward the thinner end. As the welding proceeded, melt through occurred at thicknesses lower than a certain critical thickness. If t_{max} is the critical thickness for occurrence of melt through, it is possible, by considering the equilibration forces acting on the molten metal, to determine its surface tension, through the following equation (Refs. 10–13):

$$\gamma = \frac{4.3 \times I \times E}{t_{max} \times \sqrt{Vs}} \qquad (1)$$

where, γ = surface tension (dyne/cm), t_{max} = critical thickness for occurrence of melt through (mm), I = welding current (A), E = arc voltage (V), and Vs = welding speed (cm/min).

As a reference experiment, surface tension was determined using commercial high-purity iron plates. The measured surface tension was 1500 nM/m at 14 kJ/cm heat input by this tapered plate test. This value might be slightly smaller than published data caused by purity change during experiments.

Results of Arc Spot Welding Experiments

The external appearances and the cross-sections of arc spot welds made on Steel A (no bismuth additions) and on bismuth-containing Steels C, D and E are illustrated in Fig. 3. The aspect ratio, defined as the ratio of the joint penetration depth to the spot weld diameter, is also shown for each case.

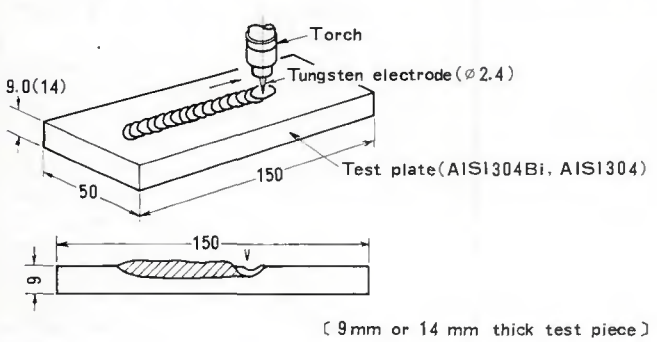

Fig. 1 — GTAW precedure for bead-on-plate experiments.

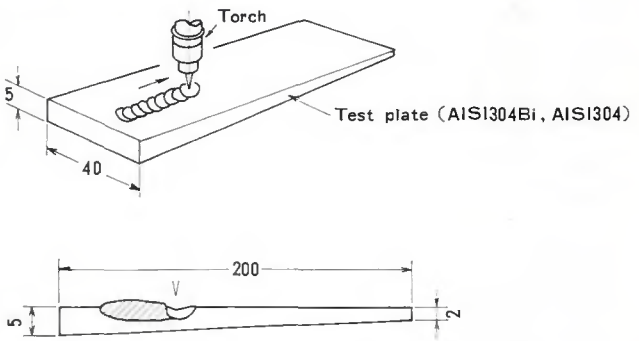

Fig. 2 — GTAW procedure for weld pool surface tension measurement using tapered test specimen.

In the case of Steel A, the weld is a shallow, peripheral penetration type of weld where the penetration is somewhat deep toward the outer periphery of the weld. In the case of Steels C, D and E containing bismuth additions, deep penetration welds (*i.e.*, the so-called simple penetration welds with a convexity at the bead bottom) are obtained. In these cases, the spot weld diameter tends to become smaller. The value of the aspect ratio was 0.19 for Steel A not containing bismuth, compared to 0.46 for Steel C with 0.04% bismuth. Steels C and D, containing 0.12 to 0.14% bismuth, had aspect ratio between 0.62 and 0.64. Thus, it can be recognized that the aspect ratio increases with increasing bismuth content.

Results of Bead-on-Plate Welding Experiments

The effect of sulfur and bismuth on weld bead formation was studied by performing bead-on-plate welding on the 9- or 15-mm-thick specimens and comparing the bead appearances and bead cross-sections. The welding current was varied from 150 to 200 A, and the welding speed from 10 to 50 cm/min. Figure 4 is an example of the results obtained.

Figure 4A shows the cross-sections of welds made with a welding current of 150 A and a welding speed of 15 cm/min (6 in./min) on specially prepared thin-plate specimens of only 4.5 mm (0.2 in.) thickness. In the case of Steel A without bismuth, a peripheral penetration type weld is observed similar to the arc spot weld mentioned earlier. In contrast, steel C, containing 0.04% bismuth, shows complete penetration, and the bead width can be observed to have become extremely narrow.

The bead appearances and bead cross-sections of welds made on 15-mm (0.6-in.) thick specimens with a welding current of 150 to 200 A at a welding speed of 20 cm/min (8 in./min) are illustrated in Fig. 4B. Here too, the trend is similar to that seen in Fig. 4A, with the bismuth-containing steels C, D and E showing deeper joint penetration (*i.e.*, larger aspect ratio) than the bismuth-free heat A.

The aspect ratio is 0.19 for Steel A compared with 0.3 or higher for Steels C, D and E. Since the states of heat conduction are different, it is not possible to compare the results of arc spot welding directly with those of bead-on-plate welding. However, it is seen that the dependency of aspect ratio on bismuth content shows a similar trend in both types of welds. Although this trend was observed to persist in general even when the welding speed was increased to 40 cm/min (16 in./min), an increasing tendency for irregular bead formation was seen in the case of the steels with higher bismuth contents.

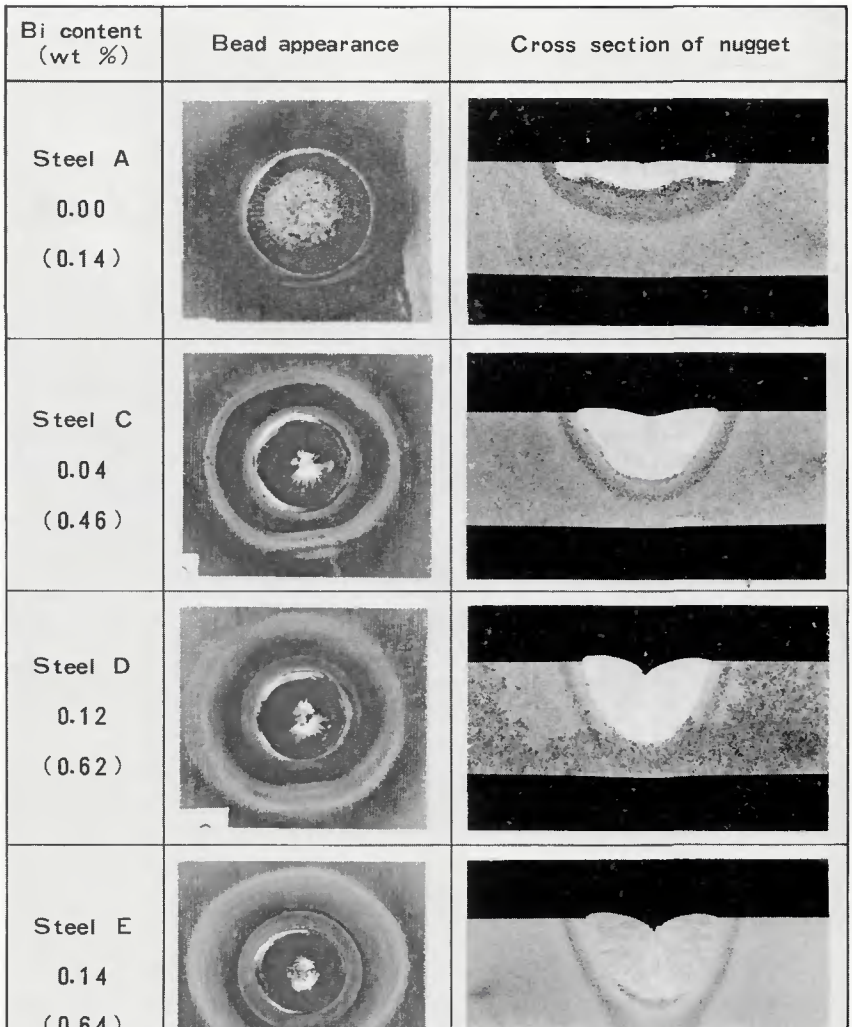

Fig. 3 — Bead appearance and macrosection of GTA spot welded AISI 304 stainless steels with various Bi contents. Note: ( ) indicates the aspect ratio defined as the ratio of penetration depth to bead width.

When the appearances of the beads shown in Fig. 4B are compared, it is seen that the bismuth-free steel forms a very stable, smooth and symmetrical bead without undercuts. In the steel with 0.04% bismuth, the bead ripples show a tendency to become slightly more coarse, but there are no visually observable discontinuities. However, in the case of Steels D and E containing more than 0.12% bismuth, the arc tends to wander, and nonsymmetrical, unsound beads with humping and undercuts were obtained. Also, due to exposure of the "dry" surface at the bottom of the crater by the arc, tunnel type pipe defects are formed as illustrated in the figure (Ref. 14).

Figure 5 illustrates the effect of bismuth content on the weld geometries of bead-on-plate welds. As shown in Fig. 5A, bismuth addition causes the bead width to become narrower by 2 to 3 mm at a welding speed of 20 cm/min. Although the bead widths increase with increasing welding current, the amount of increase is similar in both bismuth-free and bismuth-added steels. In other words, the bead widths increase by about 2.5 to 3mm (0.1 to 0.12 in.) per 100 A increase in welding current. As for the soundness of the weld bead, it was observed that bismuth additions resulted in a tendency for humping to occur at high currents and high welding speeds.

Figure 5B–C shows the crater geometries. With a welding current of 200 A, bismuth addition causes the crater

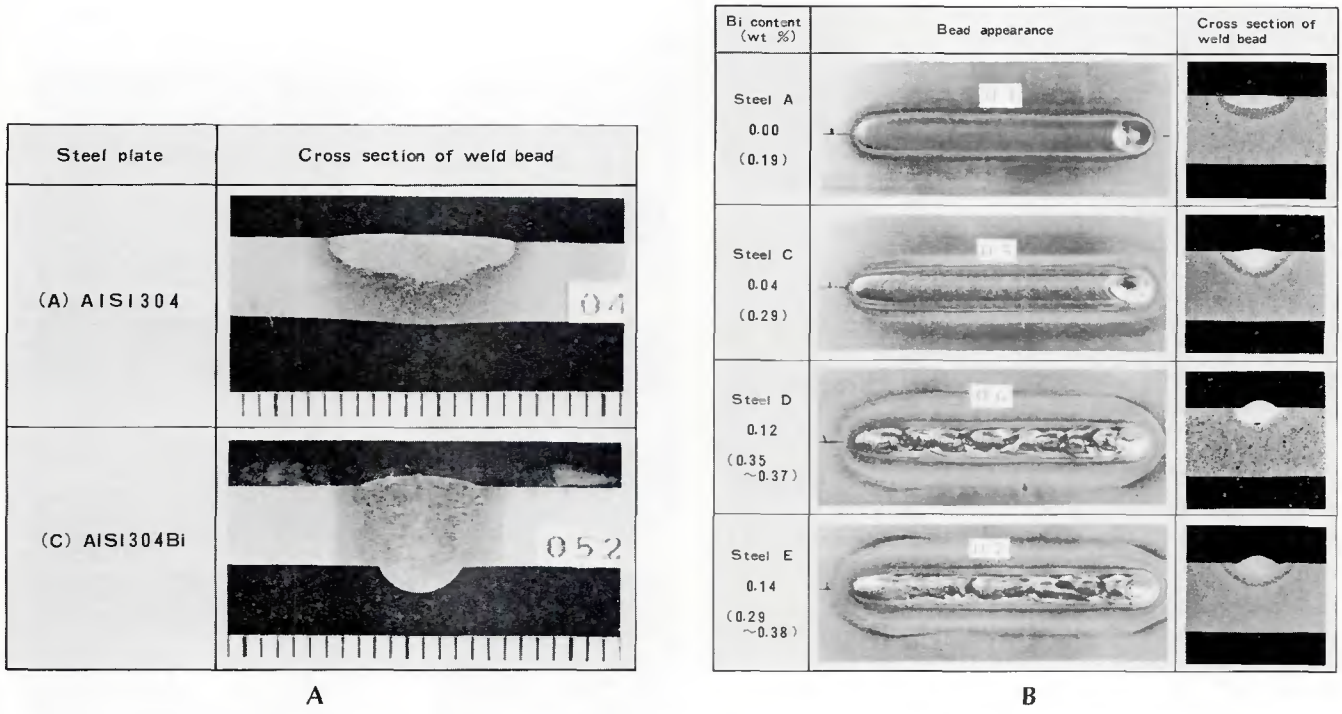

Fig. 4 — A —Macrosection of GTA bead-on-plate weld illustrating the effect of Bi on the weld joint penetration shape in AISI 304 steel. 150 A, 15 cm/min; B — bead appearance and macrosection of GTA bead-on-plate welds using 304 stainless steel with various Bi contents. Note: ( ) indicates the aspect ratio defined as the ratio of penetration depth and bead width.

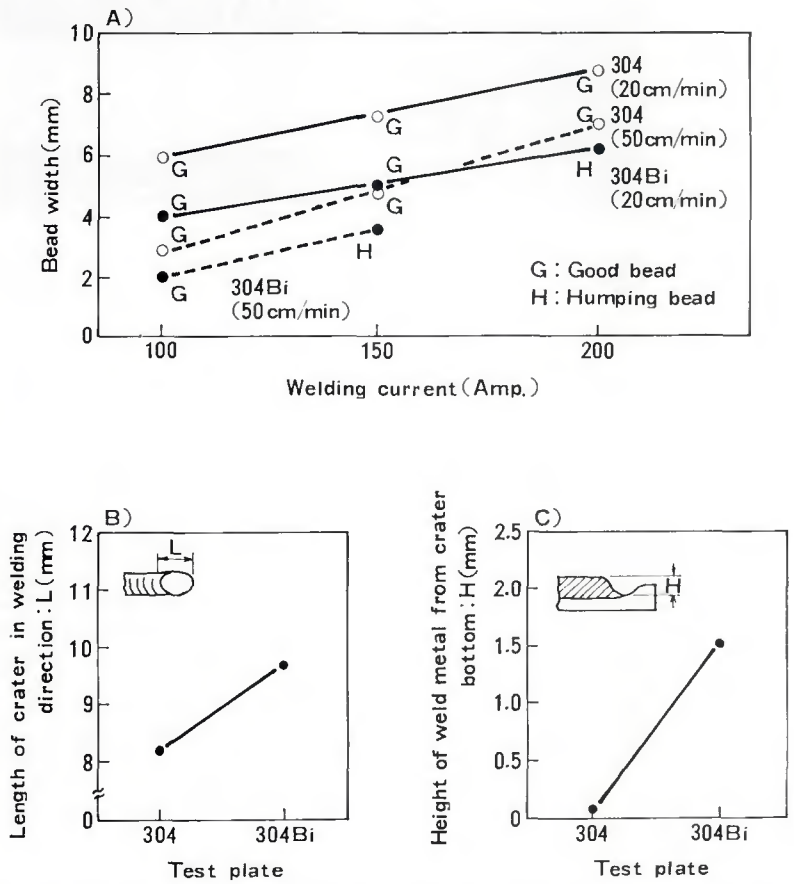

Fig. 5 — Effect of Bi contents on weld bead geometries. A — Bead width; B — length of crater; C — height of weld metal.

length L to increase. The height of weld metal from the crater bottom is also increased. Observation of the flow of molten metal during welding indicated that bismuth addition causes the molten metal wetting the surface at the bottom of the crater to be sucked back toward the rear of the crater, thus periodically exposing a "dry" crater bottom directly to the welding arc. Through observations of the bead formation process, the flow of molten metal during welding has been determined as illustrated in the drawings shown in Fig. 6.

In bismuth-free AISI 304 steel, a conduction type, a peripheral penetration weld with shallow joint penetration depth is obtained, and there is a tendency for the bead width to become large. On the other hand, in steels with bismuth additions, the molten metal is sucked back toward the rear of the crater, exposing solid metal to the arc. In addition, this molten metal flow digs into the base metal, causing the joint penetration to become deeper and the bead width to become narrower. The flow of molten metal toward the rear of the crater and exposure of the solid surface to the arc is well known to cause humping and other irregularities in bead formation (Ref. 15).

Measurement of Surface Tension Using Tapered Specimens

Welding was performed on the tapered specimens illustrated in Fig. 2 using a constant welding current of 200 A, with the welding speed varied to obtain heat inputs in the range 10 to 20 kJ/cm (4 to 8 kJ/in.), and the critical thickness for occurrence of melt through was measured. The effect of sulfur content on the surface tension is shown in Fig. 7. In the steel containing 0.001% sulfur, the surface tension, which is 1170 dyne/cm at low heat input (12 kJ/cm), decreases to 1000 dyne/cm when the heat input is increased to 20 kJ/cm. If it is assumed that the weld heat input is nearly proportional to the temperature of the molten pool, this result indicates that the surface tension decreases with increasing temperature of the molten pool. This tendency was observed to be reversed in Steel B with high sulfur content (0.03%). In this steel, the surface tension was found to increase with increasing temperature. The tendency of surface tension from this method shows the same as published data on the effect of sulfur.

It has been made clear in numerous previous studies (Ref. 8) that the effect of additions of certain elements to iron-based metals can result in a negative surface tension temperature coefficient, as in the case of aluminum additions, or in

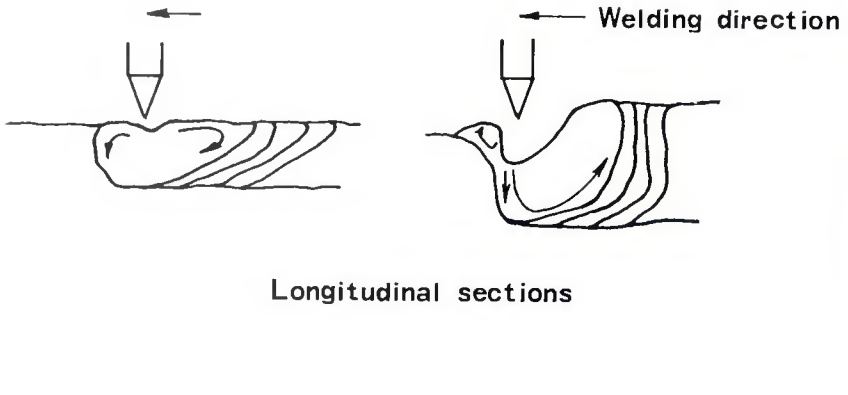

Fig. 6 — Schematics illustrating weld bead formation in the case of steels with Bi (right) and without Bi (left).

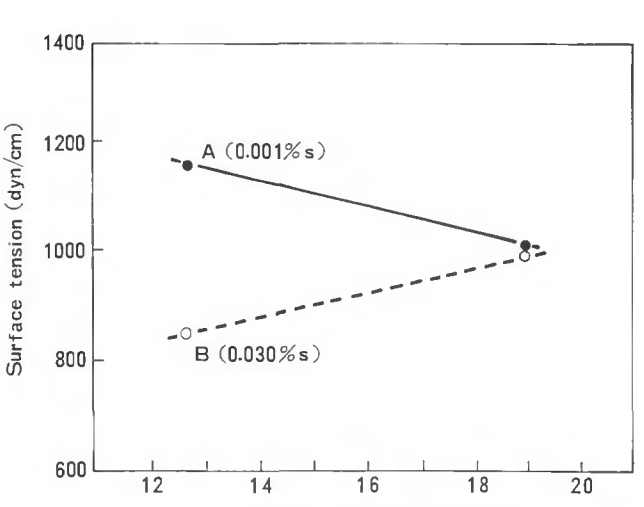

Fig. 7 — Effect of sulfur content on surface tension characteristics of GTA weld metal.

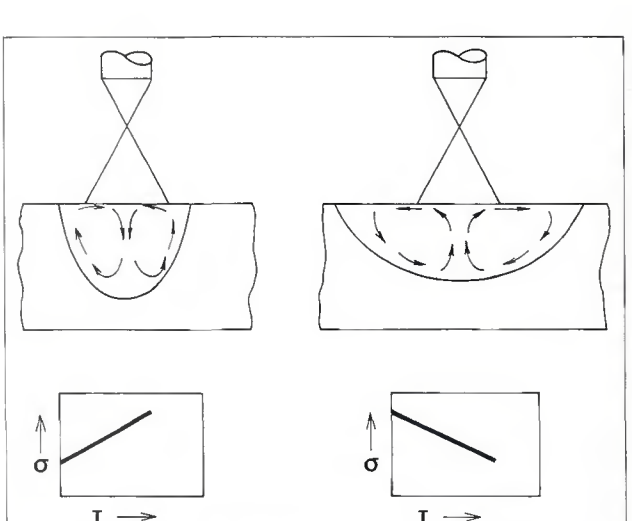

Fig. 8 — Relationship between temperature coefficient of surface tension and representative fluid flows in weld metal.

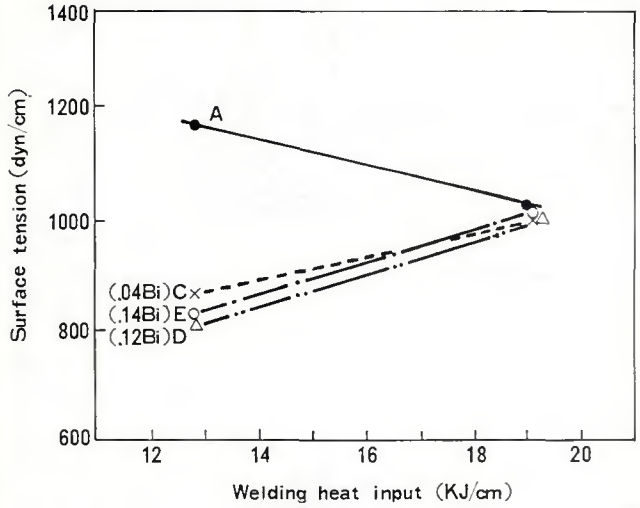

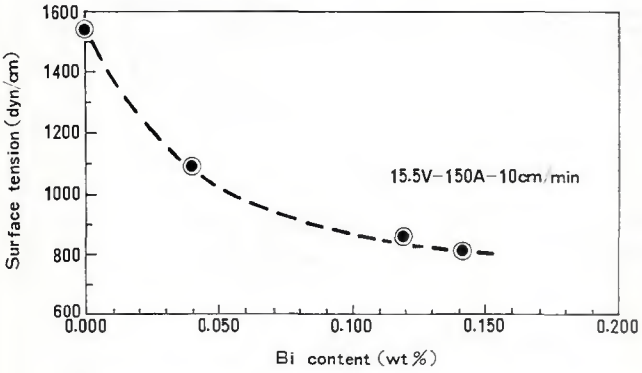

Fig. 9 — Top left: Effect of Bi content on surface tension characteristics of GTA weld metal.

Fig. 10 — Lower left: Effect of Bi content on surface tension characteristics of GTA weld metal under a heat input of 14 kJ/cm.

Fig. 11 — Below: Summary of weld bead formation with Bi in AISI 304 stainless steel.

Properties \ Test plate	AISI 304	AISI 304 Bi
Surface tension (γ)	large	small
$\frac{d\gamma}{dH}$ ($\frac{d\gamma}{dT}$)	negative	positive
Wettabitity	good	bad
Ripple on bead	fine	rough
Bead appearance	movement of molten pool; wide	narrow
Penetration	wet; shallow	dry; deep
Cross section		

a positive surface tension temperature coefficient, as in the case of sulfur or selenium additions. These trends are shown schematically in the lower part of Fig. 8.

The values for the surface tension obtained in this study seem adequately accurate even when compared to the data obtained by Heiple (Refs. 16, 17) or Kou (Ref. 18) using iron-sulfur binary alloys. Thus, if a certain amount of error could be tolerated, the method used in this study is a simple and effective method of measuring the surface tension of molten metals.

Figure 9 shows the results pertaining to the bismuth-containing steels. When the heat input is 13 kJ/cm, the surface tension of 1200 dyne/cm to the bismuth-free steel, decreases significantly to 800 to 900 dyne/cm for bismuth-doped stainless steels. However, this value does not change significantly with the amount of bismuth addition levels. When the heat input becomes greater (19 kJ/cm), the surface tension is about 1000 dyne/cm, irrespective of whether bismuth is present or not. Thus, bismuth additions result in a positive surface tension temperature coefficient, which is similar to the effect of sulfur shown in Fig. 7.

The effect of bismuth content on the surface tension characteristics under a heat input of 14 kJ/cm is shown in Fig. 10. The addition of only 0.04% bismuth to SUS 304 steel causes the surface tension to be reduced by about 30% to 1100 dyne/cm. These results indicate that the surface activity of bismuth is the same or slightly lower than that of sulfur.

Considering the results of surface tension measurements together with the results of the bead-on-plate experiments, the effect of bismuth could be explained in the following manner:

As shown in Fig. 6 and also in the upper part of Fig. 8, since the surface tension of the high-temperature portion of the pool directly under the arc is lower than that of lower temperature regions near the edges of the weld, the molten metal near the pool surface tends to flow toward the center of the weld. In addition, in the low-temperature regions, the molten metal has high fluidity. Therefore, the bead width becomes small, the joint penetration becomes deep and the bead tends to swell up. This tendency is clear in the photograph of the macrosection illustrated in Fig. 4.

Let us consider the molten metal flow across the bead cross-section in the case when the surface tension is characterized by a positive temperature coefficient. In the center of the weld where the temperature is high, the surface tension is large. Near the fusion line where the temperature is lower, the surface tension is small. Because of this, the distinctive Marangonian convective flow (Refs. 18, 19) shown in the upper part of Fig. 8 occurs, and a deep penetration weld results.

This trend is quite clearly observable in the arc spot welding series experiments (Fig. 3) as well as in the bead-on-plate welding experiments (Fig. 4). With respect to the effect of surface tension on irregular bead formation, the addition of a surface active element causes, as shown in Fig. 5, a flow of metal to occur in the longitudinal direction of the bead toward the center of the molten pool where the temperature is high and the surface tension is large. As a result, the molten metal at the crater bottom is sucked back, exposing dry solid metal to the arc. This is believed to be the cause of irregular bead formation.

Figure 11 summarizes the effect of bismuth on the GTA weldability of stainless steel. The addition of bismuth to AISI 304 steel causes a reduction in the surface tension and also causes the temperature coefficient of surface tension $d\gamma/dT$ to change from negative to positive. As a consequence of this, the bead ripples do not become coarse at low welding speeds.

The effect of bismuth on bead formation is to cause a surface tension temperature coefficient dependent Marangonian flow to occur within the weld pool which results in the molten metal at the crater bottom flowing back toward the top of the bead, leading to the formation of a narrow, deep penetration bead. This phenomenon also explains the formation of irregular beads at high welding speeds or high heat inputs.

Conclusions

The effect of bismuth additions on the weld penetration shape in GTA-welded austenitic stainless steel was investigated and the following conclusions were obtained:

Bismuth acts as a surface active element and causes Marangonian convective flow to occur within the molten pool. Because of its surface activity, the addition of bismuth results in a positive temperature coefficient of surface tension and causes the surface tension to increase with increasing heat input. Due to the above reasons, deep joint penetration occurs and there is a tendency for irregular bead formation.

Bismuth additions of 0.04% or more cause the surface tension of the molten steel to decrease rapidly. Additions of bismuth of up to 0.04% has a slightly detrimental effect on bead formation, but additions of 0.12% or more results in a tendency for irregular bead formation.

It was confirmed that the surface tension of the weld metal can be measured in a simple, but effective, manner using tapered test specimens.

References

1. Peckner, D., and Bernstein, I. M. 1977. *Handbook of Stainless Steels.* McGraw-Hill Book Co., New York, pp. 24–34.

2. Akazawa, M. 1984. Production of free machining steels with sulfur and characteristics. 98th Symposium of Nishiyama Memoriars. Iron and Steel Institute of Japan, p. 118.

3. Bhbanshu, D. 1981. New free-machining steels with bismuth. *Iron and Steel Maker* 8(3):40–44

4. Takaya. H. 1978. Recent trend of patents on free machining steels. *Electric Furnace Steel* 49(3): 210–218

5. Kimura, A., and Shibata, N. 1989. Free-machining stainless steel, DSK2UF for cold working. *Electric Furnace Steel* 60(3):292–294

6. Mizukami, H., Nagakura, Y., and Kusukawa, K. 1989. Effect of surface active element on the initial solidification structure of stainless steel ingot. *Journal of the Iron and Steel Institute of Japan* 75(8):1308–1315

7. Heiple,C. R., Roper,J. R., Stagner,R. T., and Aden,R. J. 1983. Surface active element effect on the shape of GTA, laser and electron beam welding. *Welding Journal* 62(3):72-s to 77-s

8. Keene,B. J. 1988. Review of data for the surface tension of iron and its binary alloys. *International Materials Reviews* 33 (1):1–37

9. Mills,K. C., Keene,B. J., Brooks,R. F. and Olusanya, A. 1984. The surface tensions of 304 and 316 type stainless steels and their effect on weld penetration. Proc., Centenary Conference Metallurgy Department. University of Strathclyde, Glasgow, R1-11.

10. Inagaki. K., and Okada. A. 1966. On the burn through phenomena of the thin steel plate during arc welding. National Research Institute for Metals 9(2):79–88

11. Inagaki. M., and Okada. A., 1966. Fundamental research on one-side arc welding. IIW-418-68.

12. Fujita, H., and Morita, A. 1967. On the burn through of the thin steel plate during arc welding. Nisshin Steel Technical Report 18(5) 1-13

13. Morita,A. 1970. On the burn through of the thin steel plate during arc welding 2, - Effect of alloying element, Nisshin Steel Technical Report 22(5):44–54.

14. Savage,W. F., Nippes, E. F., and Agusa, K. 1979. Effect of arc force on defect formation in GTA welding. *Welding Journal* 58(7):212-s to 224-s.

15. Lin, M. L. and Eager, T. W. 1985. Influence of arc pressure on weld pool geometry. *Welding Journal* 54(6):163-s to 169-s.

16. Heiple, C. R., and Burgardt, P. 1985. Effect of 502 shielding gas addition on GTA weld shape. Welding Journal 54(6): 159-s to 162-s.

17. Heiple, C. R., and Roper, J. R. 1981. Effect of selenium on GTAW fusion zone geometry. *Welding Journal* 60(8):143–1455.

18. Kou, S. 1987. *Welding Metallurgy.* John Wiley & Sons, New York, pp. 91–108.

19. Pollard. B., 1988. The effect of minor elements on the welding characteristics of stainless steel. *Welding Journal* 67(9): 202-s to 213-s.

Recommended Practices in Elevated Temperature Design: A Compendium of Breeder Reactor Experiences (1970–1987), Volume IV — Special Topics

WRC Bulletin 366
August 1991

Edited by A. K. Dhalla

The recommended practices for elevated temperature design of Liquid Metal Fast Breeder Reactors (LMFBR) has been consolidated into four volumes and is published in four individual WRC Bulletins.

Volume I — Current Status and Future Directions, in WRC Bulletin 362, April 1991
Volume II — Preliminary Design and Simplified Methods, in WRC Bulletin 363, May 1991
Volume III — Inelastic Analysis, in WRC Bulletin 365, July 1991
Volume IV — Special Topics, in WRC Bulletin 366, August 1991

In Volume IV, WRC Bulletin 366, special topics such as, fracture mechanics, nonlinear collapse stress classification of structural discontinuity stresses, and high-temperature design as practiced in Germany are discussed. Flaw evaluation (fracture mechanics) procedures are recommended to supplement the design codes which assume perfect, defect-free structures. The fracture mechanics methods have been extended into the plastic and creep regimes.

Publication of this Bulletin was sponsored by the Committee on Elevated Temperature of the Pressure Vessel Research Council. The price of WRC Bulletin 366 is $40.00 per copy, plus $5.00 for U.S. and $10.00 for overseas, postage and handling. Orders should be sent with payment to the Welding Research Council, Room 1301, 345 E. 47th St., New York, NY 10017.

Guidelines for Flow-Induced Vibration Prevention in Heat Exchangers

By J. B. Sandifer

WRC Bulletin 372
May 1992

The purpose of this report is to provide the infrequent user of flow-induced vibration (FIV) with enough background that he can effectively use the appropriate standard, design simple heat exchangers that are free of vibration, and effectively investigate FIV problems that arise.

Publication of this report was sponsored by the Committee on Dynamic Analysis and Testing of the Pressure Vessel Research Council. The price of WRC Bulletin 372 is $40.00 per copy, plus $5.00 for U.S. and $10.00 for overseas, postage and handling. Orders should be sent with payment to the Welding Research Council, Room 1301, 345 E. 47th St., New York, NY 10017.